

1
2
3
4

Fractal dimension of solar wind speed at different time scales using box counting method

ABSTRACT

Our investigations focused on the chaotic behavior of slow and fast solar wind through the determination of the fractal dimension at different time scales of this ionized flow that escapes from the sun towards the atmosphere. The data used to achieve this objective are solar wind speed data covering a period of twenty-five years. This is high-frequency solar wind speed data over the period 1998–2022. These data are directly extracted from the omniweb server database. the Mandelbrot method, known as box counting was adopted to calculate the fractal dimension of the solar wind speed. The frequency of occurrence of the slow solar wind is 78.61% compared to 31.39% for the fast solar wind. The fractal nature of the solar wind speed is dependent on the time scale. For the fast solar wind, the values of fractal dimension vary between 0.65 obtained in 1989 and 0.91 recorded in 2003. As for the slow solar wind, the values of the fractal dimension obtained remain more or less stable with small variations from one year to another. Although the slow solar wind has a chaotic structure and is more fractal than the fast solar wind, it has a deterministic behavior due to the invariance of its monthly fractal dimension from one month to the next.

Keywords: Wind speed, fractal dimension, box counting method, Solar wind.

1. INTRODUCTION

The Sun–Earth system is a complex system, composed of multiple interactions leading, among other things, to energy transfers from regions of the Sun to the near-Earth space environment, and in particular its magnetosphere [1, 2]. Indeed, the Sun manifests itself in the interplanetary environment following several mechanisms that affect all of space, the main ones being electromagnetic radiation and the solar wind [3]. This energy is mainly transported by the solar wind, which is a low-density plasma composed of charged energetic particles. The first explanations of the origin of the solar wind came from the American physicist Packer [1]. He made simplifying assumptions, which allowed him to obtain an equilibrium solution from the hydrodynamic equations. He concluded that the speed of the solar wind at a given distance depended on the temperature, that is, the higher the temperature, the greater the pressure gradient and therefore the faster the solar

wind. All the hypotheses he had put forward earlier were confirmed thanks to artificial satellites and space probes that were able to measure for the first time the geomagnetic field and the characteristics of the solar wind [3-6]. With the progress, the numerous investigations that followed have allowed us to know today that this flow of particles that escape from the sun contains electrons, protons and alpha particles which form an electrically neutral whole. According to [7], the characteristics of the solar wind, in particular its speed and density, vary with the nature of the sources of this wind. The two main sources of the solar wind identified in the literature are the coronal holes from which the fast solar wind ($speed \sim 700 \text{ km/s}$) emanates, and the helio which induces the slow solar wind ($speed \sim 300 \text{ km/s}$) [6]. It is important to note that the slow and fast solar winds are characterized by quite different physical parameters. For example, studies have shown that the temperature of the fast wind is higher, but its density is lower, the presence of large amplitude Alfvén waves is also frequent in the fast wind and less in the slow one [8]. Furthermore, the composition of minor species (particularly particles) is also different in these two types of wind. Thus, in many aspects, these two types of environments are quite different, even if there are some invariants [9].

The potential effects of Sun-Earth interactions are now well known and their impact on modern societies is the subject of economic estimates which justify the need for increased consideration [10]. The consequences of the space radiation environment are multiple and mainly impact space infrastructures, which can cause irreversible damage (singular events, dose effects, internal and surface charge effects, etc.). But Sun-Earth interactions can also disrupt terrestrial telecommunications, satellite positioning systems and aeronautical systems, which can therefore endanger aircraft and their passengers [11-14]. Furthermore, the consequences can extend and be observed as far as the Earth, through geomagnetically induced currents, which can, for example, damage transformers and high-voltage lines. According to [15], the effects of Sun-Earth interactions can be classified into four broad categories: effects on long conductors, on telecommunications and on aerospace infrastructures, without forgetting biological effects. In view of its effects, solar wind measurements, analyses, and interpretations are very important for better understanding the near-Earth space environment.

Most natural phenomena exhibit complex behaviors that are difficult to describe with classical methods. However, thanks to the notion of fractal dimension, introduced by [16], we can quantify this complexity. For discrete data series, this approach makes it possible to evaluate the density of information at different scales. The notion of fractal dimension constitutes the main indicator of the fractality of an object [17, 18]. It measures in some way the degree of irregularity and fragmentation of a mathematical geometric set or representing a natural object [16]. Several authors have already used this approach to analyze certain intrinsic parameters that govern the complexity of the sun-earth system. According to [19], a single fractal dimension is not always sufficient to describe the complex and heterogeneous behavior of some meteorological variables. In this case, a set of fractal dimensions must be considered [20]. Thus, if the measurement has different fractal dimensions on different parts of the medium, the measurement is multifractal [21]. For example, using solar wind data measured by the Helios 2 spacecraft in the inner heliosphere, [22] found that they exhibit a multifractal structure. Investigations conducted by [23] on daily mean solar wind speed data collected over a period of 2492 days between January 1997 and October 2003, revealed the highly fluctuating character of the solar wind, predominating over different fractal structures and singularities of different strengths. The same observations are later made by [24] on daily mean solar wind speed data collected between January 1996 and December 2006. The study carried out on the magnetic field data of the ACE satellite allowed to conclude that the presence of large-scale coherent structures during coronal mass ejections induces a decrease in multifractality compared to periods after the coronal mass ejections events [26]. Recently, [27], based on measurements of the solar wind magnetic field from the ESA-Cluster mission, analyzed the fluctuations of the solar wind magnetic field. The results suggest that the fluctuations of the magnetohydrodynamics have an intermittent character, well described in the framework of classical multifractal models [26].

In view of the above, fractal analysis is widely acknowledged today as one of the effective tools to evaluate the persistence of wind speed time series using fractal dimension as a quantitative indicator. It is therefore important to continue exploring the probable causes of the multifractality identified in the solar wind plasma because the irregular behavior of the solar wind speed observed by different authors seems to result from nonlinear dynamics rather than random external forces. This paper aims to improve current knowledge on the nonlinear dynamics of solar wind speed. More precisely, it is about determining the fractal dimension of solar wind speed over a long time series of data using the box counting method. This study will serve as a basis for the development of a simulation model for predicting solar wind speeds, essential for reducing the effects of this impressive phenomenon. Its main purpose is to improve our ability to predict geomagnetic disturbances of solar origin. After this introduction, the rest of this paper is organized as follows. In following section 2, we present the data used as well as the description of the box counting technique. The various results obtained, their analysis and their interpretations constitute the main part of section 3. Finally, we end with a conclusion in section 4.

2. MATERIAL AND METHODS

2.1 Material

The study of Sun–Earth interactions involves the observation and analysis of the solar wind. The main way to measure the state of the solar wind at different locations in the heliosphere is to use in situ instruments. Most space agencies place solar wind satellites around the Lagrange point L1, located on the axis connecting the Sun to the Earth, slightly upstream of it. This is one of the ideal points to place a satellite whose mission is to measure the parameters of the solar wind heading towards the Earth. It is often possible to access the measurements made by the different instruments directly from their Principal Investigator. In our study, we favored the use of the omniweb database. Indeed, this database, held by NASA, offers a complete history of the parameters of the solar wind, by grouping together the measurements made by the different missions that have followed one another. In addition, the data in this database are intercalibrated, and all are projected at the nose of the bow shock, in order to be spatially homogeneous. Two types of OMNI data are available: low-frequency data (time steps of one hour), and high-frequency data (time steps of the order of minutes). For our study, we used high-frequency data, more precisely solar wind speed data over the period from 1998 to 2022. Despite the presence of time holes gaps in some data time series due for example to a momentary failure of an instrument, the solar wind parameters made available on omniweb are well suited for use in data-driven models. Indeed, these time holes, when they are not too large, can be filled using different interpolation techniques.

2.2 Methods

There are several methods developed in the literature to determine the fractal dimension of an object. The best known method among them is the box method [15]. It can be applied in structures lacking the strict self-similarity property. This method can also be used for multifractal analysis.

Let T be the total observation time; it is divided into n contiguous intervals of length ε taken as successive powers of 2 ($2^0, 2^1, 2^2 \dots$). We consider the total number of occupied intervals, $N(\varepsilon)$, in which at least one value of the average solar wind speed of the time series of data used, is observed. Furthermore, we used an additional condition to calculate the same parameter for each type of solar wind. The wind speed must lower or greater than a given threshold. Thus, for the slow solar wind, $N(\varepsilon)$ represents the total number of occupied segments (or intervals) in which at least one value below 500 km/s is observed. Similarly, $N(\varepsilon)$ represents the total number of occupied segments (or intervals), in which at least one value above 500 km/s is recorded for the fast solar wind case. In case the data forms a one-dimensional fractal, then we have:

$$N(\varepsilon) \approx \left(\frac{1}{\varepsilon}\right)^D \quad (1)$$

By composing this equality with the logarithm function, we obtain the following relation:

$$\log N(\varepsilon) = -D \log(\varepsilon) + C \quad (2)$$

where D represents the fractal dimension of the series considered and C a constant. To obtain an approximation of the box dimension D we perform a linear regression on the diagram $(\log(\frac{1}{\varepsilon}), \log N(\varepsilon))$. The slope of this line provides an estimator of the fractal dimension D . Once found, the dimension D will allow us to say whether or not the object considered has a fractal structure. In fact, for D very close to 1 or 2, the object analyzed will be considered to have a Euclidean structure; on the other hand, for $1 < D < 2$, while being very far from these two values, the structure will be said to be fractal.

3. RESULTS AND DISCUSSION

2.1 Temporal variability of solar wind

Figure 1 shows the temporal evolution of the solar wind speed at a time step of 5 minutes over the entire study period. As can be seen in this figure, the values of the recorded speeds vary between 230.5 and 1076 Km/s. Wind speeds at this time scale vary greatly. However, although no clear trend emerges from this variability, there is still a significant decrease in the frequency of high wind speed values within a very specific time interval.

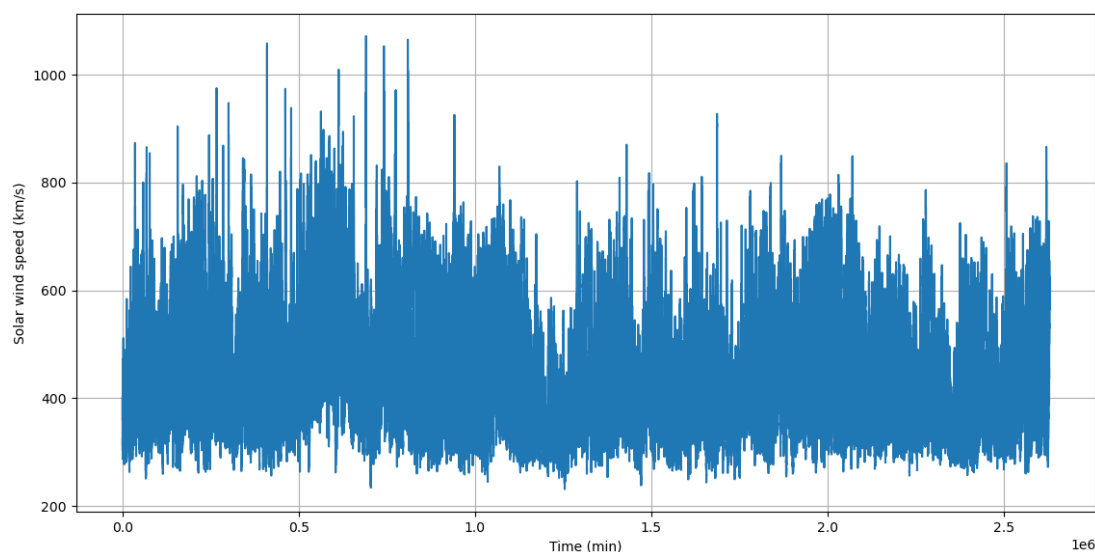


Fig. 1. Temporal evolution of solar wind speed at 5-minute steps over the entire study period.

Figure 2 illustrates the monthly variation of the solar wind speed during the study period. The analysis of this figure shows that at this time scale, the months of January, July, August and November record the maximum values with speeds exceeding 1000km/s. The lowest values of wind speed are observed during the months of September and December. This variability predominates the slow solar wind.

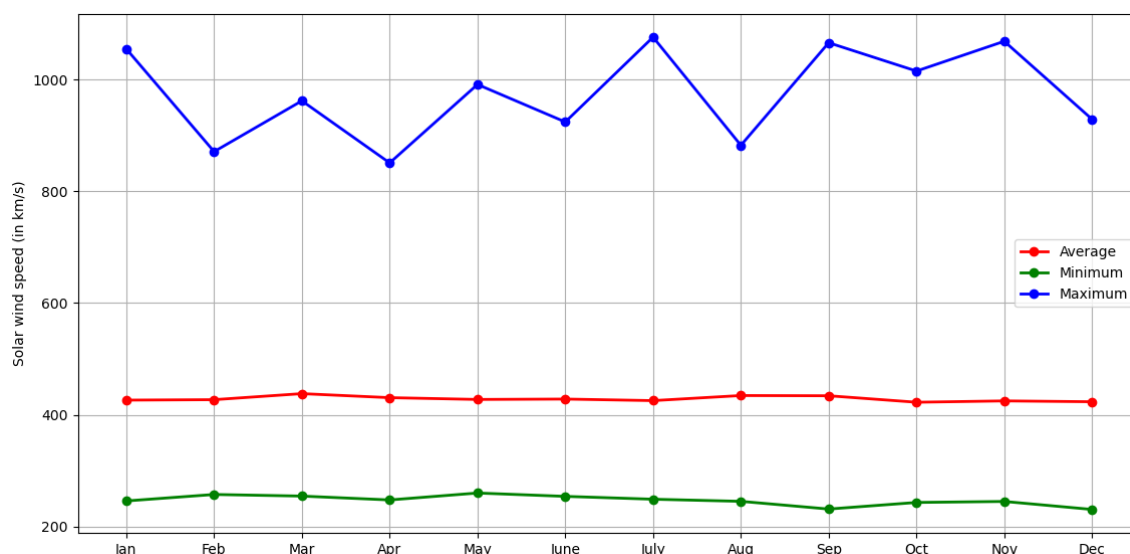


Fig. 2. Monthly variation of solar wind speed over the entire study period

Figure 3 illustrates the evolution of the minimum, average, and maximum recorded solar wind speeds for each year of the study period. The minimum speed remains relatively stable with few fluctuations. The average speed shows moderate variations over the years. The maximum speed, however, exhibits significant variations with notable peaks. These peaks are often associated with periods of intense solar activity, characterized by major events (giant solar flares, coronal mass ejections). The variations between minimum and maximum speeds reflect changes in solar wind intensity over time, influenced by coronal mass ejections. Unlike the maximum speed, the minimum speed remains nearly constant, illustrating fractal properties confined to extreme variations. The average speed acts as a stable baseline, upon which chaotic events are superimposed. Although the minimum and average speeds are stable, the maximum speed reveals a more chaotic dynamic, reflecting rare but intense events characteristic of fractal structures. The peaks in maximum speed correspond to the most chaotic and fractal phases of solar activity.

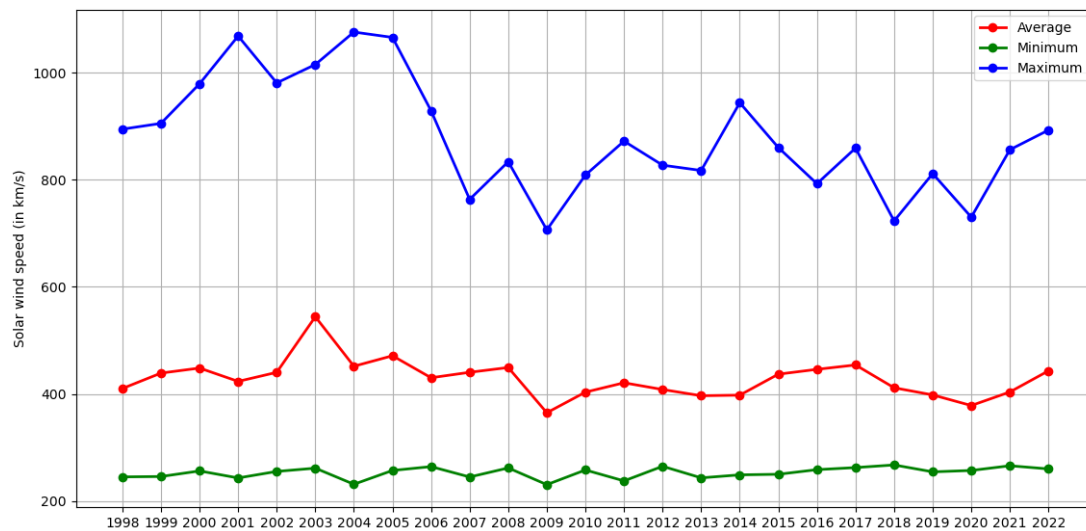


Fig. 3. Annual variation of solar wind speed over the entire study period.

The analysis of Figures 1, 2 and 3 clearly illustrate the complex and chaotic variations of solar wind, reflecting its fractal and turbulent nature. However, an in-depth analysis based on specific mathematical (or statistical) tools is required to quantify this fractality and reveal its underlying properties.

3.1 Fractal dimension of solar wind speed at different temporal Scales

According to several studies, the solar wind is described as slow when its speed is of the order of 300 km/s and it is said to be fast when its speed exceeds 500 km/s. Based on these reference values, we classified the solar winds recorded during our observation period. Figure 4 therefore presents the frequency of each type of wind observed during our study period. The analysis of this figure shows a high occurrence of the slow solar wind compared to the fast solar wind. The frequency of occurrence of the slow solar wind is 78.61% compared to 31.39% for the fast solar wind. This observation is in agreement with the conclusions of the work of [28]. The high occurrence of the slow solar wind whose density exceeds that of the fast solar wind, could be explained by the fact that it appears predominantly around the sunspot minimum because the heliosheet almost coincides with the solar equator at this period of the cycle and can sometimes reach a great thickness [7].

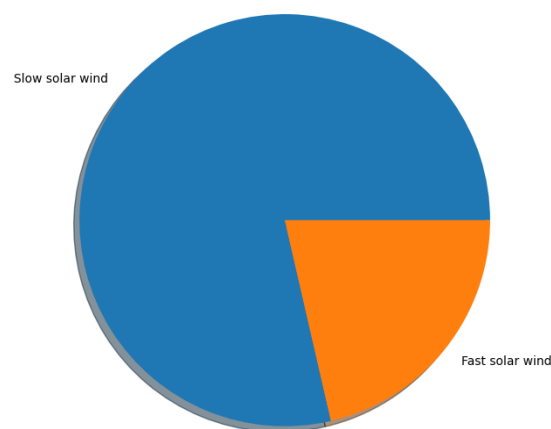


Fig. 4. Frequency of occurrence of each type of solar wind during the observation period from 1998 up to 2022.

We have evaluated in Figure 5, the effect of the time scale on the value of the fractal dimension. For this purpose, starting from the original series of one-minute data, we have constituted by aggregation, series of data of 5 min, 10 min, 30 min and one hour. The chosen method was applied to each of the series constituted and the value of the fractal dimension is determined for each of them. As can be seen in this figure, the value of the fractal dimension of the solar wind speed decreases as the time step of its measurement increases. To do this, the rest of our analyses focused on the time scale of one minute.

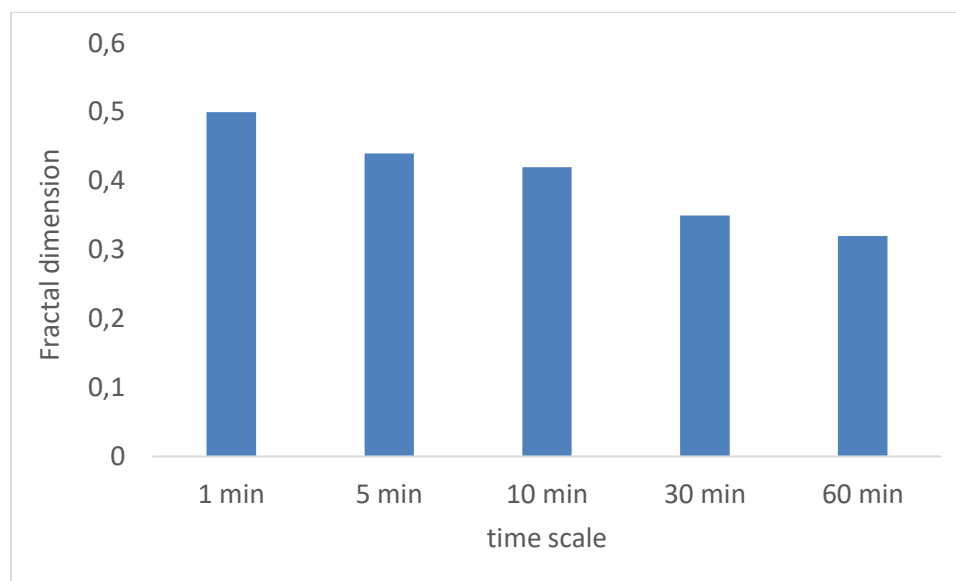


Fig. 5. Variation of the fractal dimension as a function of the time step of the time scale of measurement of the solar wind speed.

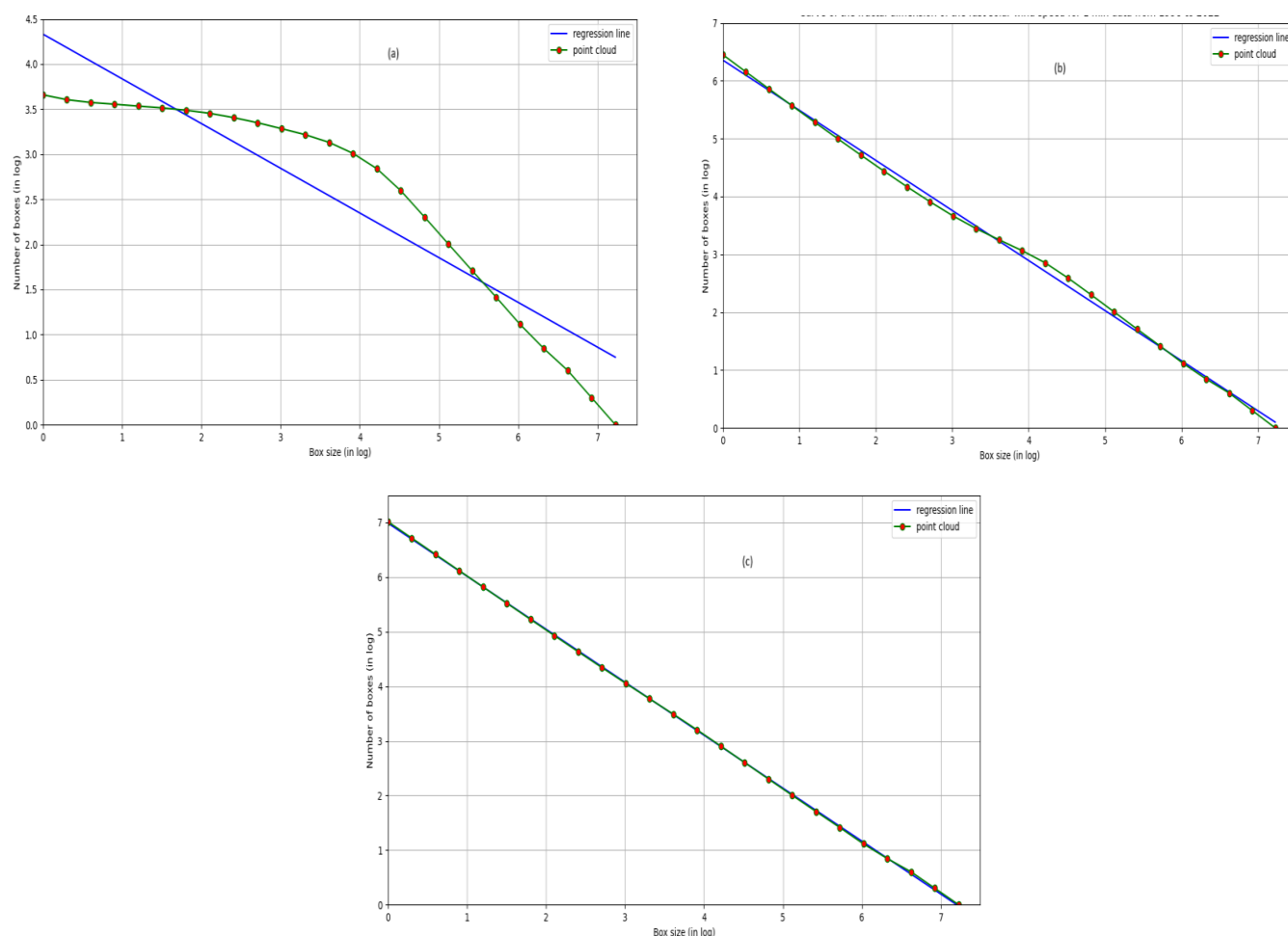


Fig. 6. $N(\varepsilon)$ versus ε for (a) all data, (b) fast solar wind and (c) slow solar wind from 1998 up to 2022.

We have represented in Figure 6 the scatter plot of the number of boxes as a function of the box sizes for the whole data set (Figure (a)), for fast solar winds (Figure (b)) and for slow solar winds (Figure (c)). According to the box counting method, the slope of the linear regression fitted to the scatterplot represents the fractal dimension of the series considered. It appears overall that the scatterplot obtained with the slow solar wind speed data are distributed linearly than the others. This shows that there seems to be some dynamics in the plasma velocity field that manages to escape by pushing and opening the magnetic field lines near the equator better than the magnetized jets in the interplanetary medium.

We have represented in Figure 7 the variability of the fractal dimension for each type of solar wind as a function of the months of the year. The analysis of this figure clearly shows that the values obtained for the slow solar wind are clearly higher than those obtained with the fast wind, whatever the month considered. The same observation is made at the monthly scale as can be seen in Figure 8. Overall, the values of the fractal dimension of the fast wind are the lowest whatever the year. For the fast solar wind, these values vary between 0.65 obtained in 1989 and 0.91 recorded in 2003. Concerning the slow solar wind, the values of the fractal dimension obtained remain more or less stable with small variations from one year to another. This result implies the existence of multifractal characteristics in solar wind speed.

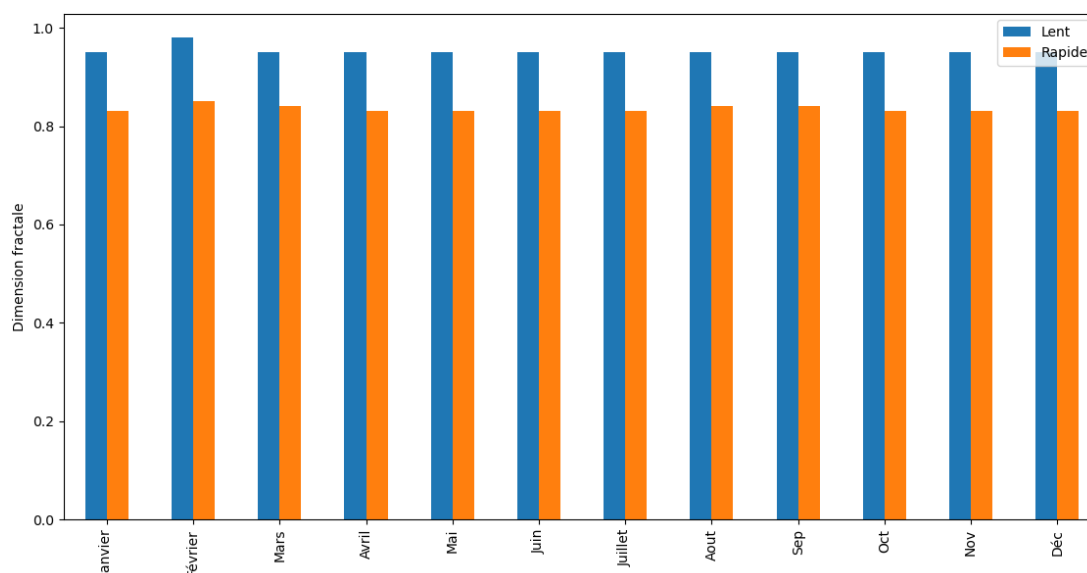


Fig. 7. Monthly variability of the fractal dimension computed for both slow and fast solar wind.

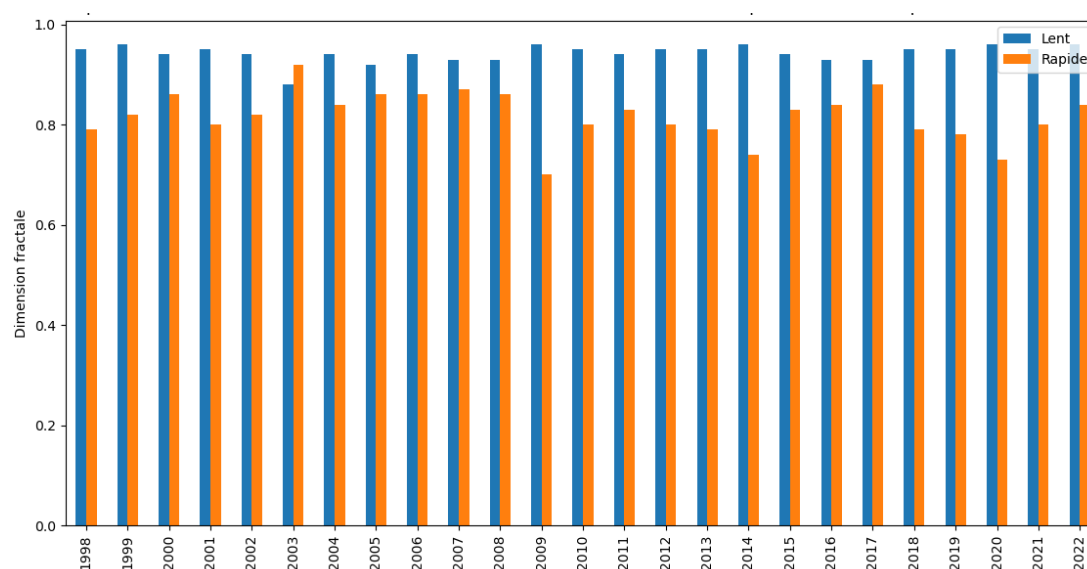


Fig. 8. Annual variability of the fractal dimension computed for both slow and fast solar wind.

273
274
275
276
277
278
279
280
281
282
283
284
285
286
287
288
289
290
291
292
293

4. CONCLUSION

In this study, we analyzed the fluctuations of the solar wind speed using the Mandelbrot method known as the box counting method through the determination of the fractal dimension of the solar wind speed at different time scales. We used high-frequency of solar wind speed data over the period from 1998 to 2022. This data is directly extracted from the omniweb server database. The technique used to compute the fractal dimension of the series considered is the box counting method. The main results of this investigation have allowed us to better understand the degree of fractal or irregular character that the solar wind plasma speed field presents. The frequency of occurrence of the slow solar wind is 78.61% compared to 31.39% for the fast solar wind. Overall, our analysis shows that during the study period, the solar wind speed exhibits chaotic behavior. The smaller the measurement time step, the more irregular the solar wind is with complex dynamics. For the fast solar wind, the values of fractal dimension vary between 0.65 obtained in 1989 and 0.91 recorded in 2003. Concerning the slow solar wind, the values of the fractal dimension obtained remain more or less stable with small variations from one year to another. These results can serve as a basis for designing simulation models and predicting solar wind speed. Moreover, whatever the time scale considered, the values of the fractal dimension of the slow solar wind are higher than those of the fast solar wind, which means that the slow solar wind is more variable and that is to say irregular than the fast solar wind. Despite this chaotic structure of the solar wind speed, a certain order of evolution of this slow solar wind speed field could be hidden there. Thus, for our next investigations, we will use more robust mathematical tools to characterize this multifractality.

311
312
313
314
315
316

REFERENCES

1. Parker, E. N., (1958). Dynamics of the interplanetary gas and magnetic fields. *Astrophys. J.*, (128), 664-676. DOI: 10.1086/146579
2. Neugebauer, M., & Snyder, C. W., (1962). Solar Plasma Experiment. *Science*, (138), 1095-1097. DOI: 10.1126/science.138.3545.1095.b
3. McComas, D. J., Barraclough, B. L., Funsten, H. O., Gosling, J. T., Santiago-Muñoz, E., Skoug, R. M. et.al. (2000). Solar wind observations over ulysses first full polar orbit. *Journal of Geophysical Research*, 105 (A5), 10,419-10,433. DOI:10.1029/1999JA000383
4. Sarkar, T., Khondekar, M. H., & Banerjee, S. (2017). Signal Processing Approach to Study Multifractality and Singularity of Solar Wind Speed Time Series. *International Journal of Information, Control and Computer Sciences*, 11(2), 168-173.
5. Youssef, M., Mahrous, A., Mawad, R., Ghamry, E., Shaltout, M., El-Nawawy, M., & Fahim, A., (2012). The effects of the solar magnetic polarity and the solar wind velocity on Bz-component of the interplanetary magnetic field. *Advances in Space Research*, (49), 1198-1202. <https://doi.org/10.1016/j.asr.2011.07.023>

317
318

319
320
321

322
323
324

325
326
327

6. Snyder, C. W., & Neugebauer M., (1964). Interplanetary solar-wind measurements by Mariner II. Proceedings of the Plasma Space Science Symposium, 67–90.
7. Legrand, J. P., & Simon, P. A. (1992). Toward a model of two-component solar cycle. *Solar Phys*, (141), 391-410. DOI: <https://doi.org/10.1007/BF00155188>
8. Weber, E. J. & Davis, L (1967). The angular momentum of the solar wind. *The Astrophysical Journal*, (148), 58-59.
9. Martin L. N., De Vita G., Sorriso-Valvo L., Dmitruk P., Nigro G., Primavera L., & Carbone V. (2013). Cancellation properties in Hall magnetohydrodynamics with a strong guide magnetic field, *Phys. Rev.*, (E 88), 063107. DOI: <https://doi.org/10.1103/PhysRevE.88.063107>
10. Upwar, D. R., Raghuwanshi S., Sondhiya, D. K., Shrivastava, R., & Jain, S. K. (2019). Multifractal Scaling of Plasma Parameters and Interplanetary Magnetic Field during Solar Cycle 23, *IJRAR*, 6(2), 31-36.
11. Val'chuk, T. E. (2004). Fractal dimension of solar wind high speed flows. *Multi-Wavelength Investigations of Solar Activity*, (223), 561-562. DOI: 10.1017/S1743921304006878
12. Chang, T. P., Ko, H. H., Liu, F. J., Chen, P. H., Chang, Y. P., Liang, Y. H., & Chen, Y. H. (2012). Fractal dimension of wind speed time series, *Applied Energy*, (93), 742-749. <https://doi.org/10.1016/j.apenergy.2011.08.014>.
13. Macek, W. M., Bruno, R., & Consolini, G. (2006). Testing for multifractality of the slow solar wind. *Advances in Space Research*, (37), 461-466. <https://doi.org/10.1016/j.asr.2005.06.057>
14. Lovejoy S., Schertzer D., & Tsoni A. A. (1987). Functional box-counting and multiple elliptical dimensions of rain. *Science*, 235(4792), 1036-1038. doi: 10.1126/science.235.4792.1036.
15. Yan, B., Chan, P. W., Li, Q. S., He, Y. C., Shu, Z. R. (2020). Characterising the fractal dimension of wind speed time series under different terrain conditions. *Journal of Wind Engineering and Industrial Aerodynamics*, (201), 3-10. DOI: 10.1016/j.jweia.2020.104165
16. Mandelbrot B. B. (1982). *The fractal geometry of nature*. W.H. Freeman and Co., New York.
17. Macek, W. M., (2007). The multifractal spectrum for the solar wind flow. *Nonlinear Processes in Geophysics*, 14(6), 695–700. <https://doi.org/10.1063/1.1618651>
18. Feng, T., Fu, Z., Deng, X., & Mao, J., (2009). A brief description to different multi-fractal behaviours of daily wind speed records over China. *Phys. Lett.*, (A 373), 4134-4141. <https://doi.org/10.1016/j.physleta.2009.09.032>
19. Consolini, G., & De Michelis, P., (2023). A Joint Multifractal Approach to Solar Wind Turbulence. *Fractal Fract.*, 7(10), 1-13. <https://doi.org/10.3390/fractalfract7100748>
20. Mandelbrot, B. B., (1989). Multifractal measures, especially for the geophysicist. *Pure Appl. Geophys.*, (131), 5–42. <https://doi.org/10.1007/BF00874478>
21. Alberti, T., Consolini, G., & Carbone, V. (2019). Multifractal and Chaotic Properties of Solar Wind at MHD and Kinetic Domains: An Empirical Mode Decomposition Approach, *Entropy*, 21(3), 320. <https://doi.org/10.3390/e21030320>
22. Macek, W. M., & Szczepaniak, A., (2008). Generalized two-scale weighted Cantor set model for solar wind turbulence. *Geophysical research letters*, 35(L02108), 1-4. <https://doi.org/10.1029/2007GL032263>
23. Salem, C., Mangeney, A., Bale, S. D., & Veltri, P., (2009). Solar wind magnetohydrodynamics turbulence: anomalous scaling and role of intermittency. *The Astrophysical Journal*, (702), 537. DOI 10.1088/0004-637X/702/1/537
24. Wirsing, K., & Mili, L., (2020). Multifractal analysis of geomagnetically induced currents using wavelet leaders. *Journal of Applied Geophysics*, 173(4), 103920. DOI:10.1016/j.jappgeo.2019.103920
25. Bolzan, M. J. A., & Rosa R. R., (2012). Multifractal analysis of interplanetary magnetic field obtained during CME events. *Annales Geophysicae*, (30), 1107–1112. <https://doi.org/10.5194/angeo-30-1107-2012>

368 26. Bolzan, M. J. A., Rosa R. R., & Sahai, Y., (2009). Multifractal analysis of low-latitude geomagnetic fluctuations.
369 Annales Geophysicae, 27(2), 569–576. <https://doi.org/10.5194/angeo-27-569-2009>

370 27. Gomes, L. F., Gomes, T. F. P., Rempel E. L., Gama S., (2022). Origin of Multifractality in Solar Wind Turbulence: the
371 Role of Current Sheets. Monthly Notices, 519(3), 3623–3634. <https://doi.org/10.1093/mnras/stac3577>

372 28. Katz, M. J. (1988). Fractals and the analysis of waveforms. Comput Biol Med, 18(3), 145-156.
373 [https://doi.org/10.1016/0010-4825\(88\)90041-8](https://doi.org/10.1016/0010-4825(88)90041-8)
374
375

376 DEFINITIONS, ACRONYMS, ABBREVIATIONS

377
378 **NASA:** National Aeronautics and Space Administration

379 **ACE:** Advanced Composition Explorer

380 **ESA:** European Space Agency

381
382
383